

Learning Low-Dimensional Embeddings for Black-Box Optimization

Riccardo Busetto¹, Manas Mejari¹, Marco Forgione¹, Alberto Bemporad²,
and Dario Piga¹

¹IDSIA Dalle Molle Institute for Artificial Intelligence, SUPSI,
Lugano-Viganello, CH name.surname@supsi.ch

²IMT School for Advanced Studies, Lucca, IT
alberto.bemporad@imtlucca.it

Abstract

When gradient-based methods are impractical, black-box optimization (BBO) provides a valuable alternative. However, BBO often struggles with high-dimensional problems and limited trial budgets. In this work, we propose a novel approach based on meta-learning to pre-compute a reduced-dimensional manifold where optimal points lie for a specific class of optimization problems. When optimizing a new problem instance sampled from the class, black-box optimization is carried out in the reduced-dimensional space, effectively reducing the effort required for finding near-optimal solutions.

1 Introduction

Black-box optimization (BBO) aims to find the solution of an optimization problem where the objective function is unknown or lacks an explicit mathematical formulation. Instead, the function can only be evaluated through queries, such as physical experiments or simulations through complex computational models. However, in many real-world scenarios, these evaluations are expensive, noisy, or time-consuming. Therefore, a key goal of black-box optimization is to find near-optimal solutions while limiting the number of costly function evaluations. Due to these challenges, BBO relies on sample-efficient strategies that select query points to balance *exploration* (searching unexplored regions) and *exploitation* (refining promising solutions). Various techniques exist for tackling these problems, including Kriging-based methods [6], Bayesian Optimization (BO) [12], Mesh adaptive

direct search [1], and recently proposed algorithms such as Set-membership approaches [10] and global optimization using inverse distance weighting and surrogate radial basis functions (GLIS) [2].

The primary limitation of the BBO algorithms mentioned above is their scalability with respect of the number of decision variables, restricting their applicability to small- to medium-size optimization problems. Black-box optimization in high-dimensional spaces still remains an open challenge, as the number of function evaluations required to cover the domain of decision variables increases exponentially with the number of dimensions. In recent years, there have been a few works to mitigate this curse of dimensionality issue, aiming at developing methods that enhance the scalability of BBO in high dimensions by exploiting different assumptions about the structure of the underlying objective function. The seminal work *Random EMbedding BO* (REMBO) [14] laid the foundation for addressing Bayesian Optimization in high-dimensional spaces. REMBO leverages the low effective dimensionality of the objective function and employs a random projection matrix to map the decision variables into a lower-dimensional subspace, where execution of BO is feasible. However, it has been shown that this approach may perform poorly even on some synthetic problems with a true low-dimensional linear subspace due to distortions introduced by the random linear projections [8]. Alternatively, the methods in [7] and [9] assume an additive structure of the objective function and decompose it into a sum of low-dimensional components, each depending on a small subset of variables. In [15], data-independent rules are explored to identify effective additive decompositions.

By leveraging the meta-learning paradigm [11], our paper focuses on reducing the dimension of the decision space where BBO is performed. Meta-learning, or “learning to learn”, involves acquiring knowledge from a class of related tasks to improve the learning process for new tasks within the same class. Following this principle, the key idea behind our approach is to learn a low-dimensional manifold where the optimal solutions of a class of similar optimization problems lie. To identify this manifold, we learn an embedding that maps the optimal decision variables of a set of problems within the considered class into a lower-dimensional latent space. This embedding is obtained using an *autoencoder* (AE) neural network, trained to minimize the reconstruction error between the optimal solutions in the original higher-dimensional space and the decoder output. The latent space of the trained AE thus serves as the desired low-dimensional representation. The problem addressed in the paper is further motivated by considering as a problem-class a multiparametric programming problem [4]. Under suitable assumptions, the optimizer can be written explicitly as a function of the parameter vector. This defines a manifold where all possible optimizers lie.

An advantage of our approach is that the optimal solutions in the original input

domain can be precomputed offline using, for example, simulators with varying parameters and computationally expensive optimization algorithms, e.g., evolutionary algorithms. This precomputed knowledge is then leveraged to solve new optimization problems by performing black-box optimization directly in the learned embedded space rather than the original higher-dimensional space. For instance, in tuning of Model Predictive Control (MPC) hyperparameters, one can first compute optimal hyperparameters using simulators of a class of parameterized systems. Then, when applying the controller to a real system, calibration is performed efficiently through experiments using BBO algorithms such as Bayesian Optimization or GLIS, searching over the precomputed embedded space rather than the original higher-dimensional domain. Although our results can be applied, in general, to any BBO method, in this paper we primarily focus on the GLIS algorithm.

2 Problem description

We consider the following *class* of optimization problems parameterized by θ

$$J(\theta) = \min_x f(x; \theta) \quad \text{s.t. } x \in \mathcal{X} \quad (1)$$

where, for a given parameter θ , $f(x; \theta) : \mathbb{R}^{n_x} \rightarrow \mathbb{R}$ is a function of the optimization vector $x \in \mathcal{X}$. The parameter θ represents a set of conditions that affect the optimization problem. These conditions may correspond to simulation settings, system configurations, or operational scenarios in real-world applications, which in turn influence the structure of the function $f(x; \theta)$. While θ is here represented as a vector in \mathbb{R}^{n_θ} , it should be understood as a description of the variations in the environment or in the system that modify the cost function, rather than merely as a vector of numbers.

We assume that an analytical expression of $f(x; \theta)$ is not available, but the function can be evaluated at any query input x and for any parameter θ . This may be the case, for instance, when θ describes different configurations of the environment and x is a design variable to be computed in order to optimize a metric f , which in turn can be evaluated only through execution of real experiments. The set $\mathcal{X} \subseteq \mathbb{R}^{n_x}$ represents known constraints on x , such as box or nonlinear constraints. The parameter θ is assumed to have a given prior distribution $p(\theta)$ from which its values can be sampled.

Let us now consider a new optimization variable $z \in \mathbb{R}^{n_z}$, with $n_z < n_x$. The problem addressed in this work is to *learn* a map $D : \mathbb{R}^{n_z} \rightarrow \mathbb{R}^{n_x}$ such that the optimization of f can be carried out effectively over the lower-dimensional variable z . Problem (1) is then transformed to:

$$J(\theta) = \min_z f(D(z); \theta) \quad \text{s.t. } z \in \mathcal{Z}, \quad (2)$$

where the embedding satisfies the constraints $\mathcal{Z} = \{z \in \mathbb{R}^{n_z} : D(z) \in \mathcal{X}\}$. A good map D should be such that the solution $x^*(\theta) = \arg \min_{x \in \mathcal{X}} f(x; \theta)$ of the original problem (1) can be recovered from the solution $z^*(\theta)$ of the reduced dimensional problem (2) as $x^*(\theta) \approx D(z^*(\theta))$.

3 Methodology

3.1 Meta-dataset creation

We generate a set of N parameters $\Theta := \{\theta^{(i)}\}_{i=1}^N$ by sampling from the prior parameter distribution, *i.e.*, $\theta^{(i)} \sim p(\theta)$. For each $\theta^{(i)}$, we solve (1) with any sample-based optimization algorithm (such evolutionary learning, MCMC with simulated annealing, GLIS) and we gather a set $\{x_k^{(i)}, f_k^{(i)}\}_{k=1}^K$ of K near-optimal vectors $x_k^{(i)}$, and the corresponding function values $f_k^{(i)} = f(x_k^{(i)}, \theta^{(i)})$, with $x_l^{(i)} \neq x_m^{(i)}, \forall l \neq m, l, m = 1, \dots, K$. For a given $\theta^{(i)}$, we refer to as near-optimal vectors as the best K candidate points explored during the iterations of the numerical algorithms used to solve (1). We denote the meta-dataset as

$$\mathcal{D} := \left\{ \theta^{(i)}, \{x_k^{(i)}, f_k^{(i)}\}_{k=1}^K \right\}_{i=1}^N. \quad (3)$$

3.2 Learning latent representation with auto encoders

An *autoencoder* (AE) is a type of neural network consisting of an encoder and a decoder, designed to learn a compressed representation of data [5]. It is trained to map an input vector $x \in \mathbb{R}^{n_x}$ to itself, while passing through a *bottleneck* layer of size $n_z < n_x$. The idea behind AEs is that the network learns a latent description of the input in a lower-dimensional latent space \mathbb{R}^{n_z} .

Let us consider an autoencoder $\mathcal{AE}_\phi : \mathbb{R}^{n_x} \rightarrow \mathbb{R}^{n_x}$ with tunable parameters ϕ , which is composed of an encoder $E_{\phi_e} : \mathbb{R}^{n_x} \rightarrow \mathbb{R}^{n_z}$ mapping x to a lower dimensional latent space vector z and a decoder $D_{\phi_d} : \mathbb{R}^{n_z} \rightarrow \mathbb{R}^{n_x}$ mapping the latent vector z to reconstruct the original vector x . Given the meta-dataset \mathcal{D} in (3), we train \mathcal{AE}_ϕ by minimizing the following weighted reconstruction error over the parameters $\phi = \{\phi_e, \phi_d\}$,

$$\mathcal{L}(\phi) = \min_{\phi} \frac{1}{N} \sum_{i=1}^N \sum_{k=1}^K w_k^{(i)} \|x_k^{(i)} - \mathcal{AE}_\phi(x_k^{(i)})\|_2^2. \quad (4)$$

Given a hyperparameter $\alpha \in [0, 1)$, the weights $w_k^{(i)}$ are defined as

$$w_k^{(i)} = \alpha^{\text{argsort}(f_k^{(i)}, \{f_h^{(i)}\}_{h=1}^K)}, \quad (5)$$

with the function $\text{argsort}(\cdot, \cdot)$ returning the index of its first argument in sorted order, from smallest to largest, with respect to the elements in the second argument. This weighting gives relatively more importance to the best candidate points $x_k^{(i)}$.

After completing the training, black-box optimization is performed over z in a lower-dimensional space. The decoder then maps the latent variable z back to the original high-dimensional space, where the function $f(x; \theta)$ is evaluated. In the following paragraph, we provide more details on the application of the proposed approach for the implementation of GLIS in a low-dimensional space. Nevertheless, the same ideas can also be applied to other BBO algorithms, such as Bayesian Optimization.

Remark 1 *In order to ensure that the autoencoder output lies within the feasible set \mathcal{X} , penalty terms can be added to the loss function in (4). Alternatively, the last layer of the decoder can be designed to enforce constraint satisfaction. For instance, in the case of box constraints, sigmoid activation functions can be used in the last layer of the decoder, and their outputs can then be rescaled based on the specified bounds.*

Remark 2 *Similarly to the discussion in Remark 1, bounds on the latent variables can also be enforced. In particular, a sigmoid activation function is used in the last layer of the encoder to rescale the latent variable z such that it belongs to the box $\mathcal{Z} = [0, 1]^{n_z}$. This restricts the search space over the latent variable domain, as discussed in the next section.*

3.3 Meta-GLIS: GLIS over a low-dimensional space

In this section, we describe how to apply the proposed methodology to implement *Meta-GLIS*—a lightweight version of GLIS based on meta learning that operates in a low-dimensional latent space. First, we recall that the encoder E_{ϕ_e} and decoder D_{ϕ_d} are pretrained (e.g., in a simulation environment) using the meta-dataset \mathcal{D} defined in (3). Given a query parameter $\bar{\theta}$ (which represents, for instance, the conditions of a real-world problem, rather than a simulated one), the goal is to solve the original optimization problem (1) for $\theta = \bar{\theta}$. Outside the simulation environment, evaluating the objective function $f(x, \bar{\theta})$ is assumed to be costly. Therefore, Meta-GLIS is expected to provide a near-optimal solution within a limited number of function evaluations.

The Meta-GLIS algorithm, summarized in Algorithm 1, follows a standard surrogate-based black-box optimization strategy. First, an initial set of samples is drawn from the latent space domain $\mathcal{Z} = [0, 1]^{n_z}$ (Step 2). The function $f(D_{\phi_d}(z), \bar{\theta})$ is then evaluated at these initial points, forming the initial dataset \mathcal{D}_M

(Step 3). In the iterative optimization loop (Steps 4), a *surrogate model* $\hat{f} : \mathcal{Z} \rightarrow \mathbb{R}$ is constructed to approximate the objective function based on the dataset \mathcal{D}_M (Step 4.1). As in GLIS, a linear combination of Radial Basis Functions (RBFs) is used to create the surrogate function, (see [2, Section 3.2]). The *acquisition function* $a(z)$ is then constructed (Step 4.2) as:

$$a(z) = \hat{f}(z) - \delta h(z), \quad (6)$$

where $h(z)$ is an exploration-promoting function, and $\delta > 0$ is a tuning hyperparameter that balances exploitation and exploration in the acquisition function. According to GLIS [2, Section 4], the exploration term is an *Inverse Distance Weighting* (IDW) function, defined as:

$$h(z) = \begin{cases} 0, & \text{if } z \in \mathcal{D}_M, \\ \frac{2}{\pi} \tan^{-1} \left(\frac{1}{\sum_{i=1}^M r_i(z)} \right), & \text{otherwise,} \end{cases} \quad (7)$$

where $r_i(z) = \frac{1}{\|z - z_i\|^2}$, with $z_i \in \mathcal{D}_M$. The acquisition function is then minimized to determine the next sampling point z_{M+1} and the corresponding decoded value $x_{M+1} = D_{\phi_d}(z_{M+1})$, at which the objective function is evaluated (Steps 4.3 and 4.4). The process continues until the maximum number of iterations is reached. The best solution is then returned.

4 Numerical examples

We evaluate the performance of Meta-GLIS on two numerical examples. The first involves the Rosenbrock function, a well-established benchmark in optimization. The second focuses on automated calibration of MPC hyperparameters. Computations are carried out on a server equipped with an NVIDIA RTX 3090 GPU. To guarantee reproducibility of the results, all Python scripts are made available in the GitHub repository <https://github.com/buswayne/meta-glis>.

4.1 Rosenbrock benchmark

In the multidimensional case, the Rosenbrock function to be minimized is defined as:

$$f(x) = \sum_{i=1}^{n_x-1} \left[\theta_1 (x_{i+1} - x_i^2)^2 + \theta_2 (\theta_{3,i} - x_i)^2 \right], \quad (8)$$

where $\theta_1 \in \mathbb{R}$, $\theta_2 \in \mathbb{R}$, $\theta_3 \in \mathbb{R}^{n_x-1}$ are random realization sampled, respectively, from the following uniform distributions $\mathcal{U}_{[10,1000]}, \mathcal{U}_{[0.1,10]}, (\mathcal{U}_{[0.1,10]}, \dots, \mathcal{U}_{[0.1,10]})$.

Algorithm 1 Meta-GLIS

Input: number of initial samples M_{init} ; maximum number of function evaluations $M_{\text{max}} \geq M_{\text{init}}$; pre-trained encoder E_{ϕ_e} and decoder D_{ϕ_d} ; query parameter $\bar{\theta}$.

1. Set $M \leftarrow M_{\text{init}}$;
2. Generate M random initial samples $Z = [z_1, \dots, z_M]$ using Latin hypercube sampling from \mathcal{Z} ;
3. Create the dataset $\mathcal{D}_M = \{z_j, f(D_{\phi_d}(z_j; \bar{\theta}))\}_{j=1}^M$;
4. **while** $M < M_{\text{max}}$
 - 4.1. Compute a surrogate $\hat{f}(z)$ of $f(D_{\phi_d}(z; \bar{\theta}))$ from \mathcal{D}_M ;
 - 4.2. Compute the acquisition function $a(z)$ (eq. (6));
 - 4.3. Compute next input sample $z_{M+1} = \arg \min_{z \in \mathcal{Z}} a(z)$;
 - 4.4. Evaluate the function $f(D_{\phi_d}(z_{M+1}; \bar{\theta}))$;
 - 4.5. Augment the dataset:
$$\mathcal{D}_{M+1} = \mathcal{D}_M \cup \{z_{M+1}, f(D_{\phi_d}(z_{M+1}; \bar{\theta}))\}$$
 - 4.6. $M \leftarrow M + 1$;
5. **end while**
6. Compute the best solution:

$$z^* = \arg \min_{z \in \mathcal{D}_M} f(D_{\phi_d}(z; \bar{\theta}))$$

$$x^* = D_{\phi_d}(z^*), \quad f^* = f(x^*; \bar{\theta})$$

Output: Best function value f^* and corresponding input x^* .

For the nominal case, $\theta = [100, 1, 1]$, the function is non-convex and has a narrow, curved valley containing the global minimum at $(x_1^*, \dots, x_{n_x}^*) = (1, \dots, 1)$.

The meta-dataset is obtained from $N = 500$ instances of the parameter θ , sampled from the uniform distributions described above, with $n_x = 20$. We solved each problem with *differential evolution* [13] with 1000 generations, and setting bounds $\mathcal{X} = [-2.5, 2.5]^{20}$ on the input domain. We then created a meta-dataset

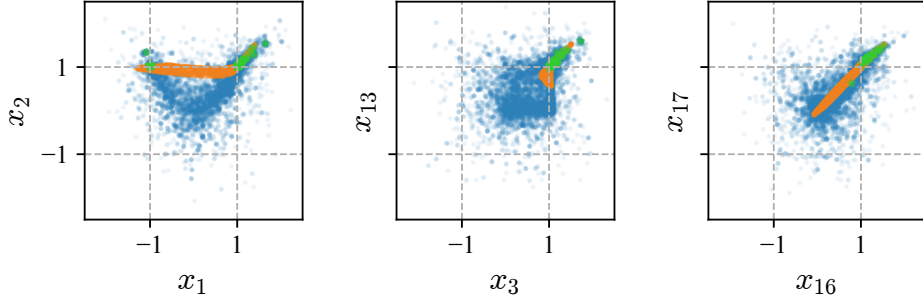


Figure 1: Learned manifold of the trained autoencoder over test functions: candidate solutions generated by the differential evolution algorithm (blue points); optimal solution for each problem instance (green points); output of the autoencoder for each candidate solution (orange points).

$\mathcal{D} = \left\{ \theta^{(i)}, \{x_k^{(i)}, f_k^{(i)}\}_{k=1}^{1000} \right\}_{i=1}^{500}$. Similarly, we generated a separate test dataset $\mathcal{D}^{\text{test}} = \left\{ \theta^{(i)}, \{x_k^{(i)}, f_k^{(i)}\}_{k=1}^{1000} \right\}_{i=1}^{100}$ to evaluate the reconstruction capabilities of an autoencoder with latent dimension $n_z = 3$, when trained as discussed in Section 3.2. The encoder and decoder are fully connected neural networks, each with two hidden layers. The encoder has n_x inputs, a first hidden layer with 128 units, a second hidden layer with 64 units, and n_z outputs. The decoder has a symmetric structure. The time required to train the autoencoder is 1229 s (approximately 20.4 minutes).

In Fig. 1 we can see the candidate solutions generated by the differential evolution algorithm (blue points), along with the optimal solution for each problem instance (green points) and the autoencoder output for each candidate solution (orange points). We can see that the reconstructed inputs lie in a manifold with reduced dispersion, which accurately describes the region where optimal solutions lie.

The Meta-GLIS algorithm is applied in the learned $n_z = 3$ -dimensional latent space, with $M_{\text{init}} = 2n_z = 6$ initial random points generated using *Latin Hypercube Sampling* (LHS) within the box $\mathcal{Z} = [0, 1]^3$. For comparison, optimization is also performed using GLIS over the original 20-dimensional input domain. In this case, $2n_x = 40$ initial points are randomly generated within the box $[-2.5, 2.5]^{20}$ using LHS. A Monte Carlo analysis is conducted on 100 newly generated problem instances that were not used for training the autoencoder.

Results are reported in Fig. 2, which shows the best value of the Rosenbrock

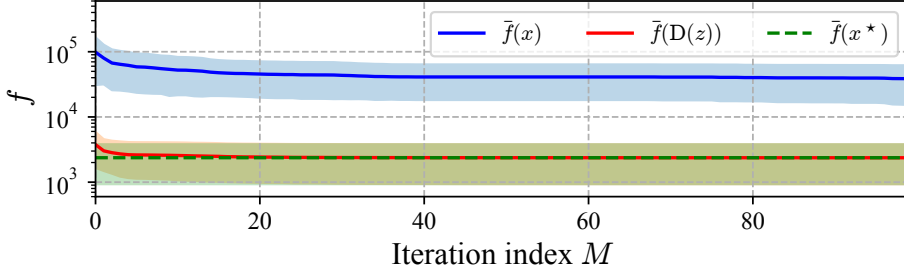


Figure 2: Comparison of the average performance obtained with GLIS (blue) and Meta-GLIS (red) over $N^{\text{test}} = 100$ runs. Global optimum (green). Shaded areas correspond to standard deviation over 100 Monte Carlo runs.

objective function achieved at each iteration of the GLIS and Meta-GLIS algorithm. The figure presents both the average and standard deviation over the 100 Monte Carlo runs. The results highlight the advantages of Meta-GLIS, which achieves near-optimal solutions after approximately 20 iterations, whereas GLIS remains far from the global optimum even after 100 iterations. This underscores the well-known advantages of running GLIS, and more in general BBO, in low-dimensional spaces.

A further analysis is provided in Fig. 3, which illustrates a single instance of the Monte Carlo runs. The figure shows the points sampled by GLIS and Meta-GLIS over the algorithm’s iterations, projected onto the same planes as in Fig. 1. It is evident that in GLIS, which directly optimizes over x , the sampled points (blue circles) after 100 iterations almost uniformly cover the search space \mathcal{X} . In contrast, in Meta-GLIS, where optimization is performed over a lower-dimensional space ($n_z = 3$) compared to GLIS ($n_x = 20$). As for the time required to fit the surrogate model, it is similar for both Meta-GLIS and GLIS (approximately 0.002 s), as it primarily depends on the number of sampled points rather than the input dimensionality.

Another advantage of Meta-GLIS over GLIS is the time required to optimize the acquisition function: on average, 0.027 s for Meta-GLIS vs. 0.149 s for GLIS. This is because the acquisition function in Meta-GLIS is defined over a lower-dimensional space ($n_z = 3$) compared to GLIS ($n_x = 20$). As for the time required to fit the surrogate model, it is similar for both Meta-GLIS and GLIS (approximately 0.002 s), as it primarily depends on the number of sampled points rather than the input dimensionality.

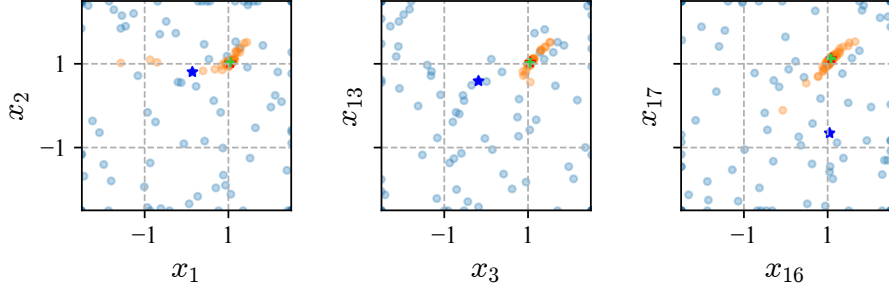


Figure 3: Sampled points by GLIS (blue circles) and Meta-GLIS (orange circles), along with corresponding best solutions (stars). The global optimal solution (green cross) overlaps with the orange star.

4.2 Automated calibration of MPC hyperparameters

We consider the same problem in [3], which uses GLIS for automatically tuning of the hyperparameters of a model predictive controller. The system to be controlled is a cart-pole described by the differential equations:

$$(M+m)\ddot{p} + mL\ddot{\psi} - mL\dot{\psi}^2 \sin \psi + b\dot{p} = F \quad (9)$$

$$L\ddot{\psi} + \ddot{p} \cos \psi - g \sin \psi + f_\psi \dot{\psi} = 0, \quad (10)$$

with p , ψ and F being, respectively, the cart position (m), the pendulum angle (rad), and the input force on the cart (N). The force F is regulated by the MPC to track a position reference p^{ref} (dashed red line in Fig. 4), while maintaining the pole in a vertical position (i.e., $\psi \approx 0$) for a pre-defined duration of the experiment T^{exp} . In addition, whenever: (i) the pendulum falls ($|\psi| > \frac{\pi}{6}$), (ii) the cart position exceeds the track length ($|p| > 1.1$ m) or (iii) numerical errors occur in solving the MPC problem, the controller is stopped at a time $T^{\text{stop}} < T^{\text{exp}}$.

For the implementation of the MPC, the continuous-time nonlinear dynamics (9) is discretized with a sampling time T_s^{MPC} , which must be greater than the time required for solving the MPC control law online $T_{\text{calc}}^{\text{MPC}}$. At each time step t , the MPC provides, with a receding-horizon strategy, the input minimizing the following objective function:

$$\begin{aligned} J_{\text{MPC}} = & \sum_{k=0}^{N_p-1} (y_{t+k|t} - y_{t+k}^{\text{ref}})^T Q_y (y_{t+k|t} - y_{t+k}^{\text{ref}}) + \\ & + \sum_{k=0}^{N_p-1} (u_{t+k|t} - u_{t+k}^{\text{ref}})^T Q_u (u_{t+k|t} - u_{t+k}^{\text{ref}}) + \\ & + \sum_{k=0}^{N_p-1} \Delta u_{t+k|t}^T Q_{\Delta u} \Delta u_{t+k|t} + Q_\epsilon \eta^2, \end{aligned} \quad (11)$$

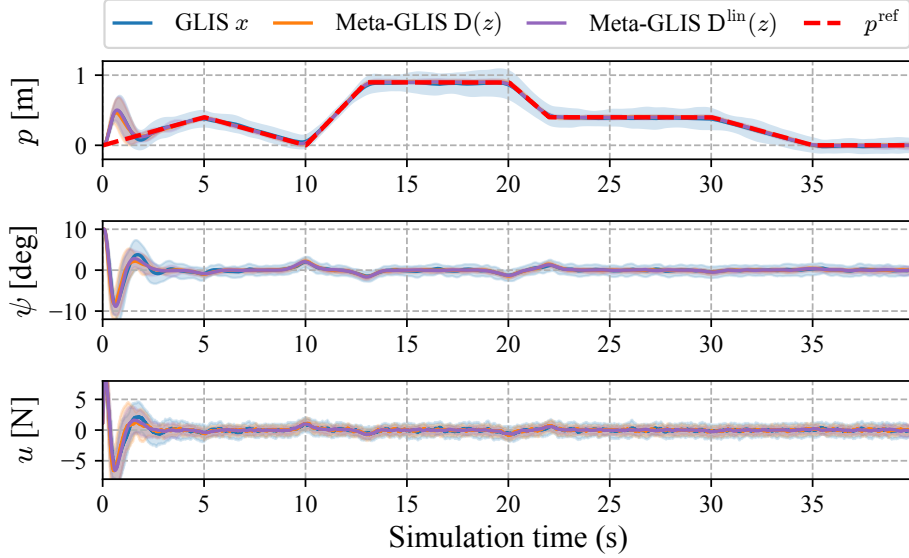


Figure 4: MPC simulation over 100 test systems: achieved performance with hyperparameters calibrated through GLIS (blue); Meta-GLIS (orange) and Meta-GLIS with linear Decoder (purple). Average (solid lines); standard deviations (shaded areas); position reference (dashed red line).

subject to input and output constraints (see [3] for details on this case study). In (11), $y = [p, \psi]$; $u = F$; N_p is the prediction horizon; u_t^{ref} and y_t^{ref} are the input and output reference; respectively, at a generic time step t ; η is a slack variable used in [3] to soften the input and output constraints; and Δu_t is the input variation.

The goal of this case study is tune the following $n_x = 14$ hyperparameters within the intervals visualized in Fig. 5: the positive semidefinite weight matrices of the MPC cost $Q_y = \begin{pmatrix} q_{y_{11}} & 0 \\ 0 & q_{y_{22}} \end{pmatrix}$, $Q_{\Delta u} \in \mathbb{R}$; prediction N_p and control horizon N_u ; MPC sampling time T_s^{MPC} ; log of the absolute and relative tolerances of the QP solver $\log QP_{\epsilon_{abs}}$, $\log QP_{\epsilon_{rel}}$ used to minimize (11); process and measurement noises of diagonal covariance matrices $W_w \in \mathbb{R}^{4 \times 4}$ and $W_v \in \mathbb{R}^{2 \times 2}$ and used by a Luenberger observer to reconstruct the system state.

The hyper-parameters calibration problem is formalized as the minimization of the following closed-loop performance index over the entire duration T_{exp} of the

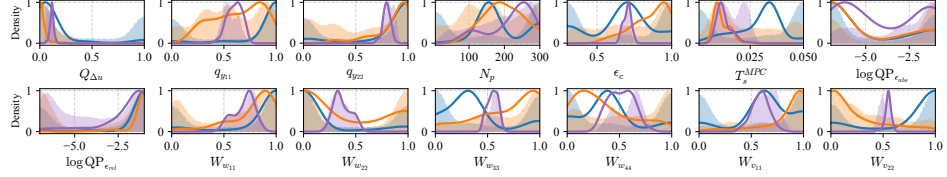


Figure 5: Empirical distributions of the optimal solutions over 100 test system realizations (solid lines) and corresponding 3000 queries sampled during the optimization (shaded areas) for each MPC hyperparameter. GLIS (blue); Meta-GLIS with nonlinear (orange) and linear decoder (purple).

experiment:

$$\tilde{J}^{\text{cl}} = \ln \left(\int_{t=0}^{T_{\text{exp}}} 10|p^{\text{ref}}(t) - p(t)| + 30|\phi(t)| \, dt \right) + \\ + \ell(T_{\text{calc}}^{\text{MPC}} - T_s^{\text{MPC}}) + \ell'(T_{\text{exp}} - T_{\text{stop}}), \quad (12)$$

where the first term penalizes the tracking error and oscillations of the pendulum, while ℓ and ℓ' are barrier functions penalizing, respectively, unfeasible real-time implementation of the control law (i.e., $T_{\text{calc}}^{\text{MPC}} \geq T_s^{\text{MPC}}$) and early stopping of the experiment (i.e., $T_{\text{stop}} < T_{\text{exp}}$).

To generate the meta-dataset \mathcal{D} , we sample the parameters $\theta = [M, m, b, f_\varphi, L]^\top$ of the cart-pole dynamics equations from distributions $[\mathcal{U}_{[0.5, 2.5]}, \mathcal{U}_{[0.2, 1.0]}, \mathcal{U}_{[0.1, 0.5]}, \mathcal{U}_{[0.1, 0.5]}, \mathcal{U}_{[0.3, 1.5]}]$, generating a total of $N = 200$ system configurations. In the generation of the meta-dataset, the cost function (12) is minimized with GLIS over 500 iterations, leading to a meta-dataset $\mathcal{D} = \left\{ \theta^{(i)}, \{x_k^{(i)}, f_k^{(i)}\}_{k=1}^{500} \right\}_{i=1}^{200}$ with $200 \times 500 = 100'000$ points. These explored points are used for training an autoencoder with the same architecture as the previous example ($n_z = 3$), with $\alpha = 0.5$.

Meta-GLIS is then applied on $N^{\text{test}} = 100$ test cases, where the cart-pole dynamics are sampled from the same distributions as those used for training. We remark that, in this case study, we assume a scenario where the meta-dataset used to train the autoencoder is constructed using synthetic data (e.g., simulators with varying settings), while Meta-GLIS should be used for hyperparameter calibration on real (and possibly time-consuming) experiments.

For a fair comparison, Meta-GLIS is evaluated against standard GLIS that also leverages information from the meta-dataset \mathcal{D} . In particular, we initialize GLIS with the optimal hyperparameter vector associated to the central parameter $\theta_0 = [1.5, 0.6, 0.3, 0.3, 0.9]$. From Fig. 6, we can see that Meta-GLIS (orange line) starts with a higher cost with respect to GLIS, but it quickly converges to cost values

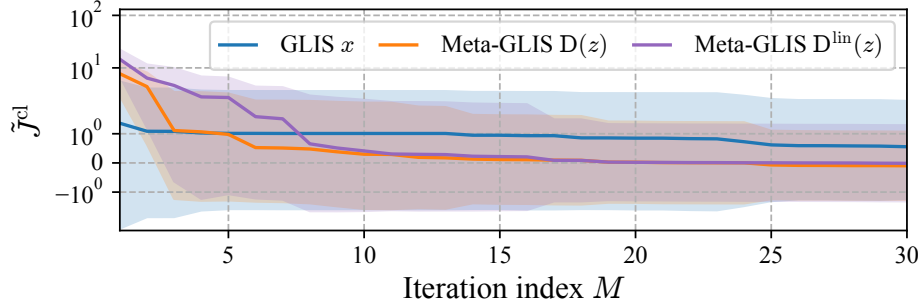


Figure 6: Closed-loop performance index \tilde{J}^{cl} vs number of algorithm's iterations. GLIS (blue); Meta-GLIS (orange); Meta-GLIS with linear decoder (purple). Average (solid lines) and standard deviation (shaded areas) over 100 system realizations.

$\tilde{J}^{\text{cl}} \leq 0$ at around iteration 20, where the cart position p has oscillations that are very small around the reference p^{ref} . This can be visualized in the simulations in Fig. 4, where the shaded areas associated to GLIS (blue) and Meta-GLIS (orange) represent the standard deviation of the trajectories over the 100 tests. Indeed, the orange shaded area is very narrow and almost coincides with the reference signal.

4.3 Linear Decoder

In order to provide an interpretation of the Meta-GLIS algorithm, we modified the architecture of the autoencoder by considering a linear decoder $D_{\phi_d}^{\text{lin}}(z)$ of the form $\hat{x} = Az + b$, with $A \in \mathbb{R}^{n_x \times n_z}$ and $b \in \mathbb{R}^{n_x}$. The structure of the encoder and the dimension of the latent variable ($n_z = 3$) are not changed with respect to the case discussed in the previous paragraph.

From Figs. 4 and 6, we can see that Meta-GLIS with linear decoder still outperforms original GLIS, with only a slight performance deterioration with respect to Meta-GLIS with a nonlinear decoder.

In Fig. 7, we can visualize the magnitude of the trained weights of the matrix A , after normalizing its columns to have norm 1. In this way, we can see which MPC hyperparameters are more sensitive to a variation of the latent variable z . From the figure, we can see that variation of z mainly influences three MPC hyperparameters, namely: N_p and the log-tolerances of the QP solver $\text{QP}_{\epsilon_{\text{abs}}}$, $\text{QP}_{\epsilon_{\text{rel}}}$.

The relevance of each MPC hyperparameter is reflected on the empirical distributions of the sampled points during the optimization and of the optimal ones. These distributions are visualized in Fig. 5. We can observe that, in the 30 itera-

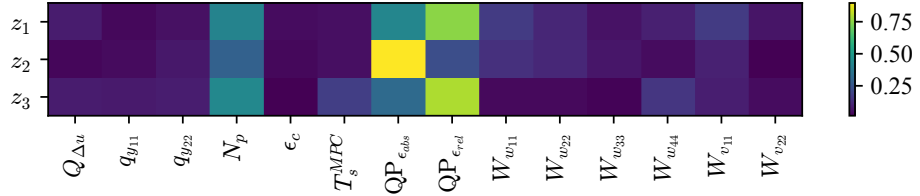


Figure 7: Magnitude of the weights of the normalized matrix A^\top characterizing the linear decoder.

tions of the algorithm, GLIS tends to sample on the bounds of the input domains (shaded blue areas). This behavior is mitigated in Meta-GLIS (shaded orange and purple areas), where the exploration is more concentrated in the region containing the optima (like in $Q_{\Delta u}$, W_v), or else is more uniform within the research space (q_y , W_{w33} , W_{v33}). Looking at the explored points when using the linear decoder, the exploration remains uniform in the search space for those hyperparameters that are more sensitive to the variation of the latent variable (namely, N_p , $QP_{\epsilon_{abs}}$, $QP_{\epsilon_{rel}}$).

5 Conclusions

We have proposed a computationally efficient method for reducing the dimension of the input space where black-box optimization is performed. The core idea of our approach is to learn a low-dimensional embedding of the decision variable space using an autoencoder trained on precomputed solutions of samples of optimization problems within a given class. These precomputed solutions can be generated, for example, via simulations with varying parameters and, if needed, through time-consuming computations. Moving from simulation to real, optimization is performed in the embedded space using experiment-driven techniques such as Bayesian Optimization or GLIS. This approach significantly reduces the number of required experiments compared to optimizing directly in the original higher-dimensional space, as we have shown through Rosenbrock benchmark and automated calibration of MPC hyperparameters.

Future work will focus on extending the methodology to experiment-driven preference-based optimization, where objective functions cannot be directly measured but are instead evaluated through qualitative comparisons between the outputs of different experiments.

References

- [1] Charles Audet and John E Dennis Jr. Mesh adaptive direct search algorithms for constrained optimization. *SIAM Journal on optimization*, 17(1):188–217, 2006.
- [2] A. Bemporad. Global optimization via inverse distance weighting and radial basis functions. *Computational Optimization and Applications*, 77:571–595, 2020.
- [3] Marco Forgione, Dario Piga, and Alberto Bemporad. Efficient calibration of embedded mpc. *IFAC-PapersOnLine*, 53(2):5189–5194, 2020.
- [4] Tomas Gal. *Postoptimal Analyses, Parametric Programming, and Related Topics: degeneracy, multicriteria decision making, redundancy*. Walter de Gruyter, 2010.
- [5] G. E. Hinton and R. R. Salakhutdinov. Reducing the dimensionality of data with neural networks. *Science*, 313(5786):504–507, 2006.
- [6] Shinkyu Jeong, Mitsuhiro Murayama, and Kazuomi Yamamoto. Efficient optimization design method using kriging model. *Journal of aircraft*, 42(2):413–420, 2005.
- [7] K. Kandasamy, J. Schneider, and B. Póczos. High dimensional bayesian optimisation and bandits via additive models. In *Proc. of the 32nd International Conference on on Machine Learning*, page 295–304. JMLR.org, 2015.
- [8] B. Letham, R. Calandra, A. Rai, and E. Bakshy. Re-examining linear embeddings for high-dimensional bayesian optimization. In *Advances in Neural Information Processing Systems*, volume 33, pages 1546–1558. Curran Associates, Inc., 2020.
- [9] P. Rolland, J. Scarlett, I. Bogunovic, and V. Cevher. High-dimensional bayesian optimization via additive models with overlapping groups. In *Proc. of the 21st Intl. Conf. on Artificial Intelligence and Statistics*, volume 84 of *Proc. of Machine Learning Research*, pages 298–307. PMLR, 09–11 Apr 2018.
- [10] Lorenzo Sabug Jr, Fredy Ruiz, and Lorenzo Fagiano. SMGO- Δ : balancing caution and reward in global optimization with black-box constraints. *Information Sciences*, 605:15–42, 2022.

- [11] Jürgen Schmidhuber. *Evolutionary principles in self-referential learning, or on learning how to learn: the meta-meta-... hook*. PhD thesis, Technische Universität München, 1987.
- [12] B. Shahriari, K. Swersky, Z. Wang, R. P. Adams, and N. de Freitas. Taking the human out of the loop: A review of bayesian optimization. *Proceedings of the IEEE*, 104(1):148–175, 2016.
- [13] Rainer Storn and Kenneth Price. Differential evolution—a simple and efficient heuristic for global optimization over continuous spaces. *Journal of global optimization*, 11:341–359, 1997.
- [14] Z. Wang, F. Hutter, M. Zoghi, D. Matheson, and N. De Freitas. Bayesian optimization in a billion dimensions via random embeddings. *J. Artif. Int. Res.*, 55(1):361–387, 2016.
- [15] J. K. Ziomek and H. Bou Ammar. Are random decompositions all we need in high dimensional Bayesian optimisation? In *Proc. of the 40th International Conference on Machine Learning*, volume 202 of *Proceedings of Machine Learning Research*, pages 43347–43368. PMLR, 2023.